

Assessment of Corrosion Damage in Steel Samples Using Electro-Magnetic Acoustic Measurements

LUKAS PETERSON¹, THANKGOD NWOKOCHA²,
ANDREI ZAGRAI¹ and T. DAVID BURLEIGH²

ABSTRACT¹

Ultrasonic thickness resonance and pulse propagation speed can be effectively used to find the thickness of thin-walled structures present in the skin of aircraft, fluid handling equipment such as pipes and in fluid storage tanks. Electromagnetic Acoustic Transducers (EMATs) yield several advantages over more traditional piezoelectric based transducers, namely that they can be used in a non-contact fashion allowing measurement regardless of surface condition or temperature. The main disadvantage of EMATs is their low efficiency. Therefore, resonance techniques, in which most of the energy is concentrated near structural resonance frequencies, are preferable to boost efficiency of electro-magnetic acoustic measurements. Thickness resonance is a technique commonly used to measure small changes in structural thickness, by integration of a ringdown curve in a wide time-domain window at different excitation frequencies. The Pulse Propagation Speed technique relies on the fact that ultrasonic waves travel faster in thicker plates in comparison to thinner plates at the same frequency. These techniques were applied to 316L stainless steel thin plates. Samples consisted of different thickness rolled material, machined samples, and samples artificially corroded with both uniform corrosion as well as pitting corrosion. These samples were used to determine the effect of thickness reduction and corrosion on the resonant peaks and lamb wave velocity. EMAT liftoff distance was also studied to quantify its effect on the amplitude, spread, and frequency of resonant frequencies and signal transition. Detectability of corrosion using EMATs was explored and quantified. Recommendations for use of EMATs for assessing corrosion damage were presented.

INTRODUCTION

Every year corrosion causes significant damage to metallic structures. While most types of metal can corrode, the type of metal where corrosion is of the most concern is in steels and other iron alloys. The type of corrosion in question usually presents as a decrease in the thickness of the metallic structural components due to uniform or pitting corrosion.

¹Lukas Peterson and Andrei Zagrai, Department of Mechanical Engineering, New Mexico Institute of Mining and Technology, Socorro, NM 87801. andrei.zagrai@nmt.edu, 575-835-5636, Fax 575-835-5209

²ThankGod Nwokocha and T. David Burleigh, Department of Materials Engineering, New Mexico Institute of Mining and Technology, Socorro, NM 87801. thomas.burleigh@nmt.edu, 575-835-5831

Several techniques have been explored to determine the thickness of steel plates namely, x-ray tomography[1], visual inspection, as well as a range of techniques utilizing the acoustic and vibrational properties of the material[2]. Techniques utilizing the vibrational and acoustic properties of samples are typically the same regardless of transducer type. Transducers that have been explored include air coupled ultrasonic transducers[3], water medium ultrasonic transducers[4], piezoelectric wafer active sensors (PWAS), and techniques using Electromagnetic Acoustic Transducers (EMATs)[2]. In thin plates, wave propagation follows guided wave principles. There are many types of guided waves that can be generated and received by ultrasonic transducers. Numerous papers have examined these wave types including, SH waves[5], LAMB waves[6], Rayleigh waves[7]. Lamb waves were chosen because they can be generated in thin plates by EMATs with little modification.

Resonance approaches are advantageous for use with EMATs as the energy is concentrated around the resonance peak, relaxing requirements for the efficiency of a transducer. In addition, resonance techniques can be used to find material properties information, sample size and damage[8], as well as additional information about the micro structure of the material such as the average grain size and crystalline orientation distribution coefficients[9], [10].

The use of EMATs to find the severity of corrosion is well accepted and documented [11]. Unfortunately, EMATs have several downsides namely, their low general efficiency, especially if ferromagnetic materials are inspected, and their dependency on the lift-off. Finally, numerous studies have shown that EMATs have an exponential decay in their efficiency as the lift-off distance increases[12].

In this study both the guided wave technique and the resonance technique are used to evaluate corrosion damage in steel samples and study the effect of the lift off.

ACCELERATED CORROSION SAMPLES

For these tests, two 316L stainless steel sheets were corroded with HCl acid. The sample labeled TGN6 was corroded with 3M HCl for 10 days, and the sample labeled TGN7 was corroded with 12M HCl vapor for 34 days. The dimensions of both of the 316L sheet samples were 0.03" x 5" x 12". The 316L sheets were cleaned with an alcohol reagent to remove dust or grease from the sample surface. The 3M HCl (TGN6) had a 50-mm diameter glass O-ring cylinder placed at the center of the stainless sheet with an O-ring between the stainless steel and the base of the cylinder. Apiezon L grease was applied generously around the O-ring and around the base of the glass cylinder to prevent crevice corrosion. The cylinder was clamped tight to the sheet with a steel clamp to prevent the solution from leaking out. The TGN6 glass cylinder was filled with 62.5 mL of 3 M HCl solution, and the top was sealed with Parafilm wax. The 3M HCl was left in contact with the stainless steel for 10 days. After 10 days, the 3M HCl was poured out, the sample was rinsed with DI water, cleaned with a plastic bristle brush, and the grease was removed with acetone. The sample was viewed on a Hirox K7700 digital microscope and uniform corrosion was observed on the surface that was in contact with the 3M HCl. The corroded sheet is shown on the left of Figure 1.

The vapor corrosion test used the vapor from an open flask of concentrated (12M)

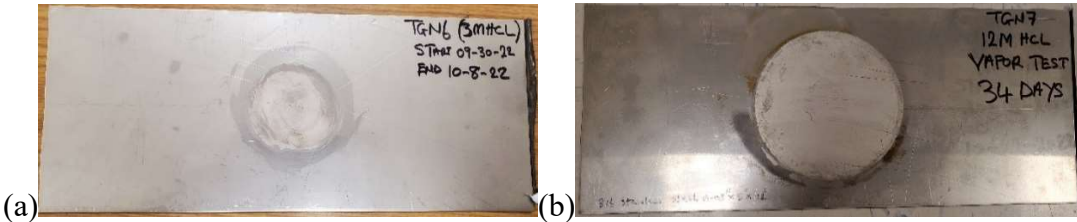


Figure 1. Photos of (a) TGN6 and (b) TGN7 accelerated corrosion samples.

HCl. The surface of the 0.03" x 5" x 12" 316L stainless steel sheet was cleaned with alcohol as described above. Next a 25-mL Erlenmeyer flask was placed in the center of the sheet. This flask was filled with 10 mL of 12M HCl and left open. A larger 75-mm diameter glass O-ring cylinder tube was placed over the small flask. The base O-ring was also generously greased with Apiezon L grease. The open top was sealed with Parafilm wax to prevent escaping of the vapor. The HCl vapor was left in contact with the 316L sheet for 34 days. Afterwards, the glass vessels were removed, and the stainless steel was cleaned as before and examined with the Hirox optical microscope, and uniform corrosion was also found on the surface. The vapor corroded sheet is shown on the right of Figure 1.

GUIDED WAVES SPEEDS AND RESONANCES IN STEEL PLATES

The speed at which an ultrasonic lamb wave propagates through a thin plate is dependent on several factors namely the pressure wave speed, the sheer wave speed, signal frequency, and plate thickness. In thin plates, symmetric and anti-symmetric Lamb waves can be generated and analyzed. The symmetric or S mode dispersion curves can be found by solving Equation 1 while the antisymmetric or A mode dispersion curves can be calculated by solving Equation 2[17]. Generally in equations 1 through 4 d is the plate thickness, ξ is the symmetric or antisymmetric eigenvalues, and finally p and q can be found using equations 3 and exist purely to simplify notation.

$$\frac{\tan pd}{\tan qd} = -\frac{(\xi^2 - q^2)^2}{4\xi^2 pq} \quad (1), \quad \frac{\tan pd}{\tan qd} = -\frac{4\xi^2 pq}{(\xi^2 - q^2)^2} \quad (2)$$

Solving these transcendental equations numerically yields the dispersion curves. Instabilities in numerical solution cause deviation of data as the curves approach an asymptote. These unreliable data points were removed to better define resonance asymptotic seen for the A1 mode at 2 MHz and 2.5 MHz in Figure 2Figure 1.

$$p^2 = \frac{\omega^2}{C_p^2} - \xi^2, \quad q^2 = \frac{\omega^2}{C_s^2} - \xi^2 \quad (3) \quad C_g = C^2 \left(C - fd \frac{\partial C}{\partial (fd)} \right)^{-1} \quad (4)$$

Finally, the group velocities can be found using Equation 4, where C_g is the group velocity, C is the phase velocity, d is the plates thickness, and f is the frequency. The result of calculation for steel plates of two thicknesses is presented in Figure 2

It can be seen from Figure 2 that at least two corrosion detection strategies are possible. The first one utilizes a differences in sound speed for plates of different thickness. These sounds speeds can be measured directly using a pitch-catch wave propagation method. The second approach relies on the resonance behavior of the

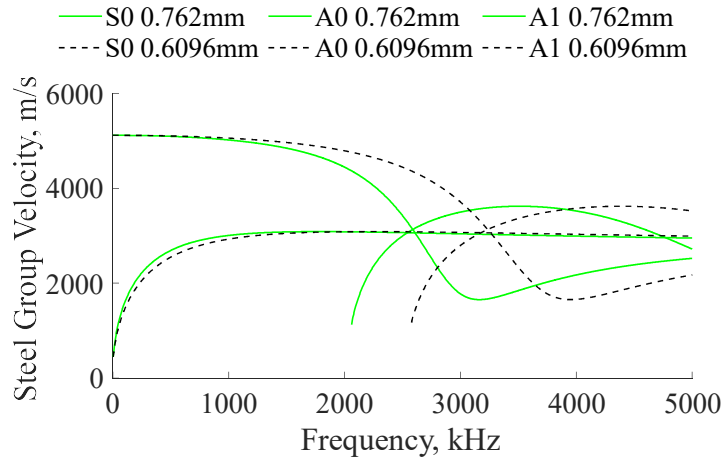


Figure 2. Dispersion curve for steel 316l plates of various thicknesses.

plate at and around the asymptotes of the group velocities seen in Figure 2. Due to the constructive interference of both the original signal and the signals reflected from the top and bottom surfaces of the plate, the resonance behavior is observed and the frequency of the resonance could be used for the detection of corrosion damage.

ULTRASONIC ASSESSMENT OF CORROSION DAMAGE IN STEEL PLATES

The experimental equipment used for both wave propagation and resonance approaches consisted of a RITEC RAM-5000, a RITEC RT-50, a pair of EMATs, and a National Instruments PXIe-5142 in a PXIe-1062Q (for guided wave experiments). The RITEC RAM-5000 generated ultrasonic signal which was then amplified to be fed into RT-50 Ohm impedance matching unit to ensure 50 Ohms of resistance on the transmission EMAT in spite of its true resistance. The EMATs used were a pair of custom made low frequency Lamb wave EMATs consisting of a coil, a neodymium magnets embedded in epoxy surrounded by steel shielding. The National Instruments PXIe-5142 in a PXIe-1062Q chassis was used to record and digitize transmitted and received waveforms with 14-bit precision for the guided wave experiments. For the resonance testing, an additional superheterodyne receiving circuit was used in RITEC RAM-5000. Superheterodyne receivers enables adding an oscillator signal to the received signal resulting in constructive interference for similar frequencies and destructive interference for signals with dissimilar frequencies. The resultant signal at each sweeping frequency is then integrated over a specific time window to yield a frequency spectrum indicative of the resonance behavior.

Resonance technique

In resonance experiments, one EMAT was placed underneath each steel plate while another EMAT was placed on top of the plate, allowing alignment of the EMATs to maximize detection signal. A pair of EMATs in this configuration were

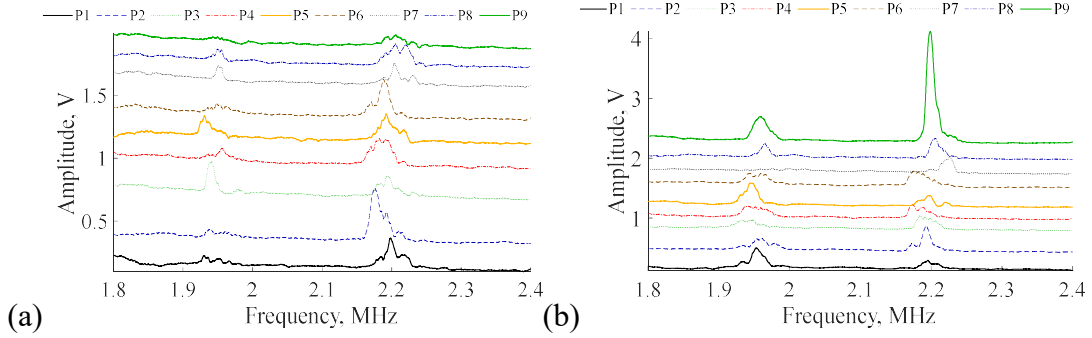


Figure 3. Resonance test results for (a) TGN6 sample and (b) TGN7 sample.

placed at semi-random locations on the plate. Boundary conditions were implemented by having a steel plate resting on foam blocks.

The RITEC RAM-5000 high pass filter was set to 1 MHz, the low pass filter was set to 20 MHz, and the amplifier was set as 40 dB. The gated integrator gate delay was set as 210 μ s, the gate width was set at 50 μ s, and the integration rate was set at 2000 V/Vms. The frequency scan was conducted between 1.8 MHz and 2.4 MHz with an increment of 100 Hz at a rate of 10 bursts/second. The output signal was set at the level of 80 with a burst width of 200 μ s. Due to the initially noisy resonance data, a 101 point moving average was applied in post processing yielding much cleaner spectra.

The results for TGN6 plate can be seen on Figure 3a and the results for the TGN7 plate can be seen on Figure 3b. Locations 1 through 6 (P1-P6) are located over pristine parts of the plates while the remaining three points are over the corroded regions of the plates (P7-P9). There is a small but recognizable tendency for the peaks to shift to a higher frequency by 17.1 kHz in TGN6, 24 kHz in TGN7. This shift must be considered in light of measurement repeatability in each location on the plate. Should this technique be deployed, high measurement stability is recommended.

The larger frequency shift in TGN7 correlates with a more pronounced corrosion damage in this sample. Of note is the impressive amplitude of the location 9 (P9) peak in the TGN7 experiment due to being located in the center of the corroded region.

Guided waves technique

In the guided wave experiments, the EMATs were installed in a 3D printed jig designed to keep the EMATs exactly 6 inches apart (center to center). The jig with the EMATs was placed on top of the center of the plate which was then placed on the foam.

The RITEC RAM-5000 high pass filter was set to 100 KHz, the low pass filter was set to 20 MHz, and the amplifier was set as 40 dB. The frequency was set at 400 KHz, the burst width was set at 3.0 cycles, the burst delay was set at 1.6125 μ s, and the phase was set at 0 degrees. The output level was set at 100 while the burst rate was set at 10 bursts/second. A bandwidth filter set between 100 Hz and 2.5MHz. 100 sample averaging was used to obtain a recorded signal. In addition, a moving average was allied to reduce signal noise.

The results can be seen below in Figure 4. This signal shows first a transmitted signal appearing due to the electromagnetic interference which is followed by a direct S0 wave mode is visible at approximately 30 microseconds on Figure 4. Further wave modes and reflections were observed in the raw data but were omitted for clarity of presentation. The use of the amplitude of received signals is mostly consistent and is therefore not a good candidate for corrosion detection as surface microstructure can affect guided wave amplitude. A slight phase delay, on the order of tenths of a microsecond, was observed in the corroded samples yielding a potential path forward for corrosion detection in steel structures. This is consistent with the theoretical dispersion curves that were calculated as the delay grows with corrosion depth.

EFFECT OF LIFT OFF DISTANCE

Effect of lift off in Resonance technique

One of the EMATs was placed under the sample while the other EMAT was placed in a 3D printed liftoff jig that also contained an Acuity A100 laser distance sensor to determine liftoff. The magnets contained within the EMATs were used to align the transducers while the experimental settings are identical to those used in the

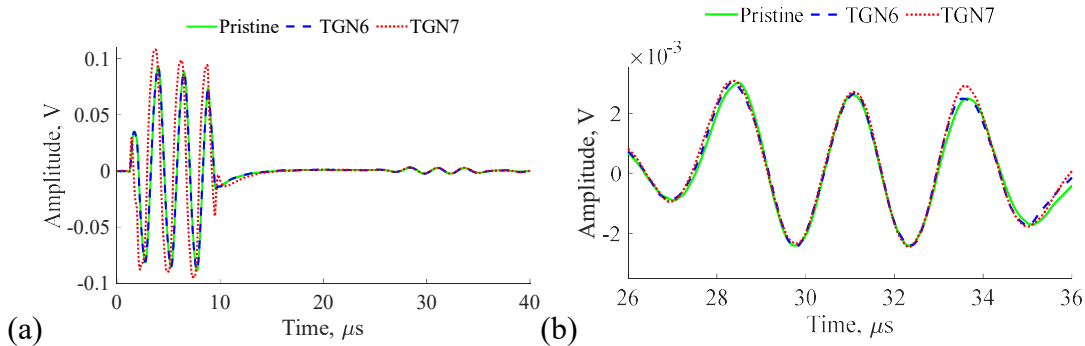


Figure 4. Guided waves received after propagation through various levels of corrosion.

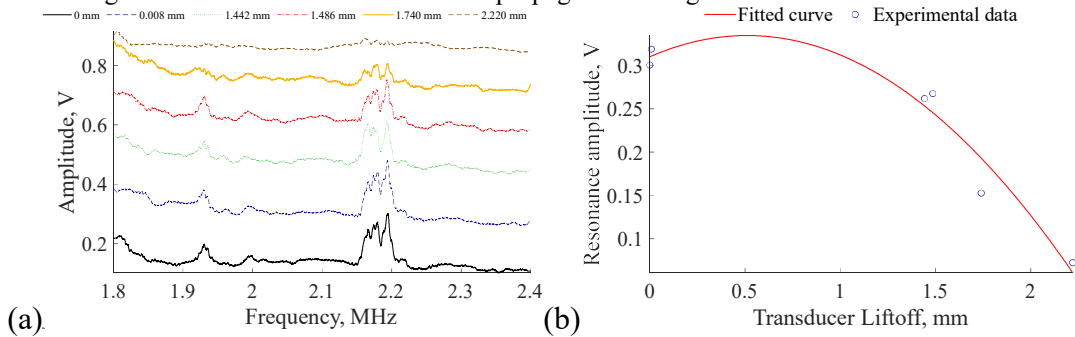


Figure 5. Experimental analysis of the effect of EMAT liftoff on resonance technique.

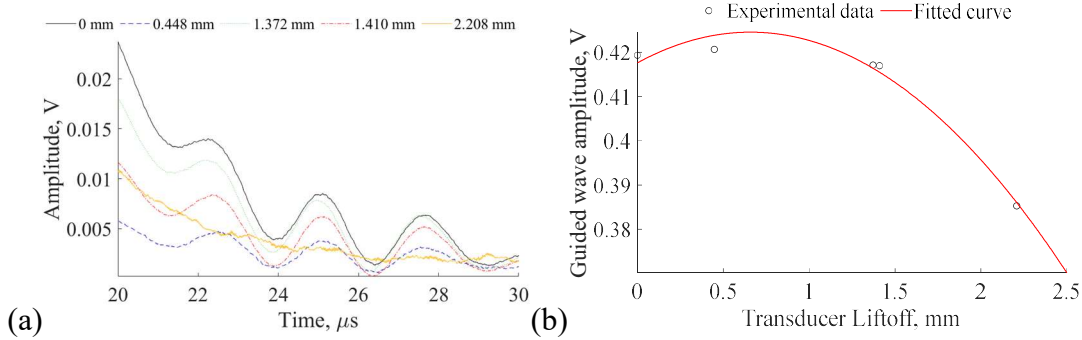


Figure 6. Experimental analysis of the effect of EMAT liftoff on guided wave technique.

resonance technique to quantify corrosion damage. Starting at the lowest liftoff distance resonance experiments were conducted between 0 and 5 millimeters without changing EMAT location in relation to the plate. The results seen in Figure 5 show that as the EMATs are lifted from the plate the transducers have an exponential decrease in transducer efficiency. The equation describing the curve in Figure 5 is $Liftoff = -0.09375 * Amplitude^2 + 0.0959 * Amplitude + 0.31$.

Effect of lift off in Guided Wave technique

Both of the EMATs were placed in the 3D printed liftoff jig along with the laser distance sensor to verify the liftoff distance. Once again starting at the lowest liftoff distance guided wave experiments were conducted between 0 and 5 millimeters without moving the sample plate. Similar to the resonance liftoff experiment the guided wave liftoff experiment shows an exponential decay in signal amplitude as EMAT transducer liftoff rises. The equation describing this decay seen in Figure 6 is $Liftoff = -0.01602 * Amplitude^2 + 0.02109 * Amplitude + 0.4176$. The guided wave amplitude values seen on the right of Figure 6 were found by subtracting the minimum value between 25.8 μ s and 26.8 μ s from the maximum value between 24.6 μ s and 25.6 μ s.

CONCLUSIONS

A pair of 316L stainless steel plates were artificially corroded with Hydrochloric acid. These plates along with a pristine sample were used to detectability of corrosion using the resonance and guided wave corrosion quantization methods. The resonance method is excellent at quantifying small changes in thickness but breaks down should the plate have any surface roughness, as is the case with heavy corrosion, causing the ultrasonic waves to disperse instead of constructively interfere or should the sample have any unknown geometry. The guided wave showed a less detectable difference in signals, rendering the guided wave method better suited to detecting heavy corrosion where surface roughness would disrupt the resonance method or for detecting corrosion over the entire path of the guided wave. EMATs show an exponential decay in efficiency when removed from the samples surface but are

useable up to around 1.75 mm for resonance technique while the guided wave method is usable with liftoff up to around 1.5 mm of liftoff.

ACKNOWLEDGMENTS

This work was performed, in part, through support by the National Nuclear Security Administration NA-191 program funding.

REFERENCES

- [1] C. Wang *et al.*, “Determination of thickness and air-void distribution within the iron carbonate layers using X-ray computed tomography,” *Corros. Sci.*, vol. 179, p. 109153, Feb. 2021, doi: 10.1016/j.corsci.2020.109153.
- [2] W. Luo and J. L. Rose, “Guided wave thickness measurement with EMATs,” *Insight - Non-Destr. Test. Cond. Monit.*, vol. 45, no. 11, pp. 735–739, Nov. 2003, doi: 10.1784/insi.45.11.735.52961.
- [3] G. Waag, L. Hoff, and P. Norli, “Air-coupled ultrasonic through-transmission thickness measurements of steel plates,” *Ultrasonics*, vol. 56, pp. 332–339, Feb. 2015, doi: 10.1016/j.ultras.2014.08.021.
- [4] L. Mountassir, T. Bassidi, and H. Nounah, “Experimental study of the corrosion effect on the elastic properties of steel plates by ultrasonic method,” *Phys. B Condens. Matter*, vol. 557, pp. 34–44, Mar. 2019, doi: 10.1016/j.physb.2019.01.008.
- [5] X. Zhang, X. Liu, B. Wu, C. He, T. Uchimoto, and T. Takagi, “An improved analytical model of the magnetostriction-based EMAT of SH0 mode guided wave in a ferromagnetic plate,” *Ultrasonics*, vol. 108, p. 106213, Dec. 2020, doi: 10.1016/j.ultras.2020.106213.
- [6] K. Rieger, D. Erni, and D. Rueter, “Unidirectional emission and detection of Lamb waves based on a powerful and compact coils-only EMAT,” *NDT E Int.*, vol. 122, p. 102492, Sep. 2021, doi: 10.1016/j.ndteint.2021.102492.
- [7] H. Liu *et al.*, “Design and experiment of array Rayleigh wave-EMAT for plane stress measurement,” *Ultrasonics*, vol. 120, p. 106639, Mar. 2022, doi: 10.1016/j.ultras.2021.106639.
- [8] P. Wang, Y. Zhang, E. Yao, Y. Mi, Y. Zheng, and C. Tang, “Method of measuring the mechanical properties of ferromagnetic materials based on magnetostrictive EMAT characteristic parameters,” *Measurement*, vol. 168, p. 108187, Jan. 2021, doi: 10.1016/j.measurement.2020.108187.
- [9] B. Ahn, S. Seok Lee, S. Taik Hong, H. Chul Kim, and S.-J. L. Kang, “Application of the acoustic resonance method to evaluate the grain size of low carbon steels,” *NDT E Int.*, vol. 32, no. 2, pp. 85–89, Mar. 1999, doi: 10.1016/S0963-8695(98)00032-2.
- [10] M. D. G. Potter, S. Dixon, and C. Davis, “Development of an automated non-contact ultrasonic texture measurement system for sheet metal,” *Meas. Sci. Technol.*, vol. 15, no. 7, pp. 1303–1308, Jul. 2004, doi: 10.1088/0957-0233/15/7/011.
- [11] M. Gori, S. Giamboni, E. D’Alessio, S. Ghia, and F. Cernuschi, “EMAT transducers and thickness characterization on aged boiler tubes,” *Ultrasonics*, vol. 34, no. 2–5, pp. 339–342, Jun. 1996, doi: 10.1016/0041-624X(95)00093-I.
- [12] J. He, S. Dixon, S. Hill, and K. Xu, “A New Electromagnetic Acoustic Transducer Design for Generating and Receiving S0 Lamb Waves in Ferromagnetic Steel Plate,” *Sensors*, vol. 17, no. 5, p. 1023, May 2017, doi: 10.3390/s17051023.